Chinese Chemical Letters 36 (2025) 110318

Contents lists available at ScienceDirect

Chinese Chemical Letters

journal homepage: www.elsevier.com/locate/cclet

Dual-ligand engineering over Au-based catalyst for efficient acetylene hydrochlorination

Yongsheng Xu[a], Lisha Yao[a], Jian Li[c], Yanzhao Dong[a], Dongyang Xie[a], Miaomiao Zhang[a], Feng Li[a], Yunsheng Dai[c,*], Jinli Zhang[a,b], Haiyang Zhang[a,*]

[a] School of Chemistry and Chemical Engineering/State Key Laboratory Incubation Base for Green Processing of Chemical Engineering, Shihezi University, Shihezi 832000, China
[b] School of Chemical Engineering and Technology, Tianjin University, Tianjin 300354, China
[c] Yunnan Precious Metals Lab Co., Ltd., Kunming 650106, China

ARTICLE INFO

Article history:
Received 5 June 2024
Revised 25 July 2024
Accepted 5 August 2024
Available online 6 August 2024

Keywords:
Acetylene hydrochlorination
Gold-based catalyst
Dual-ligand engineering
Catalytic performance enhancement

ABSTRACT

Introducing ligand into the surface of gold (Au)-based catalyst has been recognized as an efficient strategy to enhance the performance of catalyst in acetylene hydrochlorination reaction. However, due to the multifactorial deactivation, the usage of single type of ligand has limitations on the performance improvement. In this work, two types of ligands including a molecular 2-methylimidazole and an ionic cetrimonium are selected to protect Au^{n+} species. After kinetics analysis, advanced characterization, and density functional theory simulation, we demonstrate the optimal interaction model between two ligands and Au species: Two 2-methylimidazole molecules are coordinated with high-valent Au species while cetrimonium is interacted *via* electrostatic interaction. Except the synergistic effect in the decrease of Au species reduction and agglomeration, the existence of molecular ligand greatly increases the adsorption of hydrogen chloride while the ionic ligand significantly inhibits the deposition of coke. Due to the positive effect of dual-ligands, we achieved 97.1% of acetylene conversion and 0.29 h^{-1} of deactivation rate under high gas hourly space velocity of acetylene. This work establishes a foundation to explore the property-activity relationships in Au-based catalyst *via* ligand engineering.

© 2025 Published by Elsevier B.V. on behalf of Chinese Chemical Society and Institute of Materia Medica, Chinese Academy of Medical Sciences.

Since 1950s, mercury as the main active component has been used to catalyze the acetylene hydrochlorination to produce vinyl chloride monomer (VCM) in China [1]. Due to the severe pollutant resulting from mercuric volatilization and the assignment of Minamata accord, a replacement for mercury-based catalyst in the acetylene hydrochlorination reaction should be mandated [2,3]. In 1985, G. J. Hutchings correlated the catalytic activity of supported metal chloride catalysts to draw the conclusion that Au should be the best catalyst for this reaction theoretically [4]. During the past decades, the experiments about Au-based catalyst in acetylene hydrochlorination reaction have proved the above prediction [5-16]. As same as other metal-based catalysts, the Au-based catalyst still suffers from the deactivation because of coke deposition, chlorine poison, metal reduction and agglomeration [17,18]. Combining the fact with the increasing prices of Au, how to increase and then keep the activity during the reaction is still a challenge in this field.

As we all known, the environment of metal active site depends on the activity and stability of heterogeneous catalyst [19-21]. To improve the performances of Au-based catalyst, many efficient strategies have been developed by researchers *via* the modification of support, the design of multi-metallic components or the introduction of ligands on the surface of catalyst. For example, through heteroatom doping into activated carbon, the electron density of the metal center is controlled and the electron transfer between active site and support is promoted, thus improving the performance of acetylene hydrochlorination reaction [22-24]. By contrast, more and more researchers have been focused on the determination of ligands introduction due to its abundance, such as inorganic salt, organic molecules, ionic liquid and so on [25-28]. Usually, a single ligand is used in catalyst preparation to balance the protection and exposure for active sites. For example, Hutchings' lab has played more attention on the inorganic salt containing sulphur to form the Au-S complexes, which is contributed to better immobilization of oxidized Au^{n+} during the reaction [29]. Zhao *et al.* used [Bmim][$N(CN)_2$] as a ligand to enhance the adsorption of hydrogen chloride *via* the formation of Au–[$N(CN)_2$–]

* Corresponding authors.
E-mail addresses: daiysh@ipm.com.cn (Y. Dai), zhy198722@163.com (H. Zhang).

https://doi.org/10.1016/j.cclet.2024.110318
1001-8417/© 2025 Published by Elsevier B.V. on behalf of Chinese Chemical Society and Institute of Materia Medica, Chinese Academy of Medical Sciences.

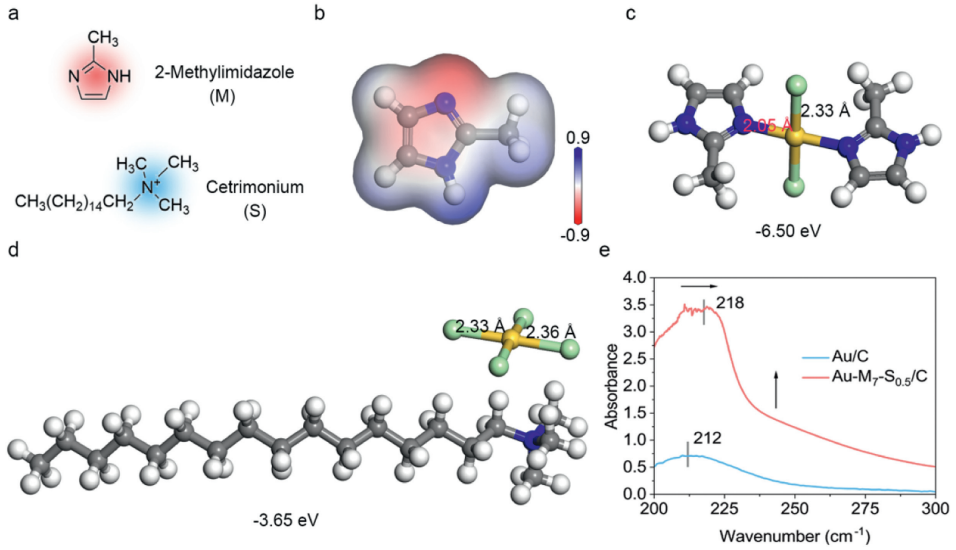

Fig. 1. (a) Structures of two ligands. (b) ESP of ligand M. (c) Optimal simulated model between $AuCl_x$ and ligand M. (d) Optimal simulated model between $AuCl_x$ and ligand S. (e) UV-vis spectra of Au/C-W and Au-M_7-$S_{0.5}$/C. C atom: gray; H atom: white; N atom: blue; Au atom: yellow; Cl atom: green.

complexes, suggesting the advantage of the ionic ligand in this reaction [30]. Zhang *et al.* selected two molecule ligands containing N-P-O elements to weaken the adsorption of acetylene over Au-based catalyst [31]. Based on above analysis, it is found that the Au-based catalyst is optimized through different pathway with different types of ligands. Moreover, the performance of catalyst in this reaction depends on many factors, such as the chemical state of Au species, the adsorption of reactants.

Inspired by the difference enhancement of single ligand, there was an idea that whether could we introduce the more types of ligands into catalyst surface to achieve positive effects of these ligands simultaneously. In this study, two types of ligands including a molecular 2-methylimidazole (denoted as M) and an ionic cetrimonium (denoted as S) were selected and then introduced into activated carbon-supported gold (Au/C) in preparation process. After kinetics analysis, advanced characterization, and density functional theory (DFT) simulation, we assessed the optimal interaction model between two ligands and Au species: Two 2-methylimidazole molecules were coordinated with high-valent Au species while cetrimonium was interacted *via* electrostatic interaction. Then, the roles of ligands in the activity and stability enhancement were determined through analyzing the fresh and spent Au-based catalysts and adsorption of reactants. Due to the positive effect of dual-ligands, we achieved 97.1% of acetylene conversion and 0.29 h^{-1} of deactivation rate under high gas hourly space velocity (GHSV) of acetylene. The work establishes a foundation to explore the property-activity relationships in Au-based catalyst *via* ligand engineering.

Two types of ligands, including a molecule of 2-methylimidazole and a cation of cetrimonium, are selected in this work (Fig. 1a). DFT simulations were first employed to clarify the optimal interaction between Au metal site and ligands. From the electrostatic surface potential (ESP) of ligand M (Fig. 1b), we can demonstrate that the electrons are enriched on N atom unbonded to hydrogen atoms, which provides more opportunity to coordinate with the dsp^2 hybridization of Au^{3+}. After simulation (Figs. S1 and S2 in Supporting information), the structure, in which the two chloridions are substituted by two ligand M molecules, shows the lowest formation energy with -6.5 eV (Fig. 1c), suggesting the optimal structure between $AuCl_x$ and ligand M. Due to the coordination, the bond distance of Au-N decrease to 2.05 Å, shorter than Au-Cl in $[AuCl_4]^-$ (2.35 Å, Fig. S3 in Supporting information). That is, this coordinated structure between Au metal site and ligand M is more favorable than $[AuCl_4]^-$ from thermodynamics. As for ligand S, the optimal structure is achieved through the electrostatic interaction with $[AuCl_4]^-$ (-3.65 eV, Fig. 1d) rather than the coordination (Figs. S4 and S5 in Supporting information). To directly demonstrate the interaction between these two ligands and Au^{3+}, the ultraviolet-visible (UV-vis) spectrum in solution was employed. The $HAuCl_4$ solution shows a weak characteristic peak at 212 nm (Fig. 1e), which is assigned to the d-d transition of Au^{n+} species. While after adding ligands with the relative molar ratio, the intensity significantly increases and the peak is red shifted to 218 nm, suggesting that the existence of interaction increases the ratio of Au^{n+} species.

The dispersion of Au site over prepared catalysts were investigated by high resolution transmission electron microscope (HRTEM) and X-ray diffraction (XRD). Compared with Au/C (Fig. 2a), we demonstrate that the aggregation of Au site over Au-M_7-$S_{0.5}$/C is obvious reduced (Fig. 2b), in which the particle size decreases from 3.46 nm to 2.45 nm (insets of Figs. 2a and b). The XRD patterns of the catalysts are further shown the greater dispersion of Au sites after dual ligands protection due to the low intensity of diffraction peaks attributed to metal Au (PDF #65-2870, Fig. 2c). Also, the increased intensity in Au/C pattern may be caused by higher self-reduction of Au ions. So, the chemical states of Au are studied through the Au 4f regions in X-ray photoelectron spectroscopy (XPS) (Figs. 2d and e). Both three chemical states, including Au^0, Au^{1+}, and Au^{3+}, exist in the prepared catalysts while the content of oxidized Au^{n+} (Au^{1+} and Au^{3+}) shows obvious differences. Oxidized Au^{n+} accounts for ~56% in Au-M_7-$S_{0.5}$/C while only 27% in Au/C (Table S1 in Supporting information), suggesting that the introduction of these two ligands is beneficial to inhibit the reduction of Au species over activated carbon. In particular, there is obvious overstatement of Au^0 species in both Au-M_7-$S_{0.5}$/C and Au/C, which is caused by observable beam-induced photoreduction in XPS characterization. Besides, the H_2-temperature programmed reduction (TPR) was employed to further determine the chemical state of Au species. The reduction peak temperatures of Au^{3+} and Au^+ for Au/AC catalysts are 230 °C and 318 °C, respectively [30]. However, after ligand coordination, the intensity of peaks both increases and then the relative reduction peaks are shifted to 282 °C and 403 °C (Fig. 2f). The higher intensity suggests the high content of Au^{n+} species in fresh catalyst, whose results are consistent with XPS spectra. The backward shift of the reduction peak temperature indicates that this dual-ligand engineer-

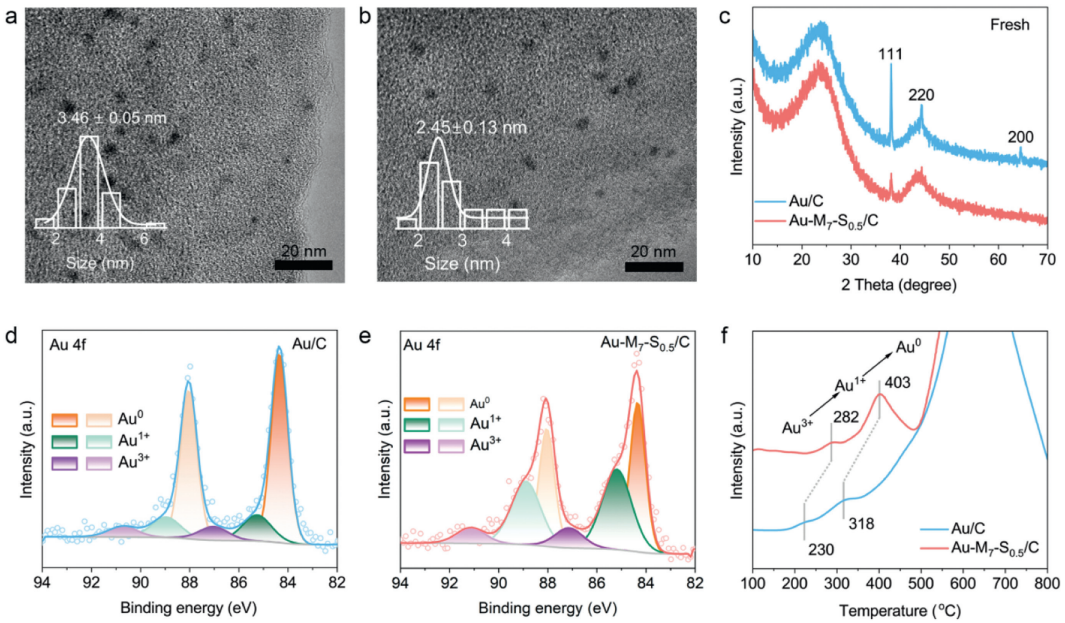

Fig. 2. HRTEM images of (a) Au/C and (b) Au-M_7-$S_{0.5}$/C; Insets are the size analysis plots of Au species. (c) XRD patterns of Au/C and Au-M_7-$S_{0.5}$/C. Au 4f regions of (d) Au/C and (e) Au-M_7-$S_{0.5}$/C. (f) TPR profiles of Au/C and Au-M_7-$S_{0.5}$/C.

ing can make the oxidized Au state of the catalysts more stable at high temperatures. All above results, including great dispersion, high proportion of Au^{n+} species, and more stable at reduced atmosphere, both indicate that this dual-ligands engineering is beneficial for promoting the activity of Au-based catalyst in acetylene hydrochlorination.

The catalytic performances were evaluated and then compared for the acetylene hydrochlorination reaction in a fixed-bed reactor with the same conditions. Due to the deactivation of catalyst, we introduced two descriptors containing deactivation rate and selectivity loss rate (details in Supporting information). The two gold-based catalysts without ligand addition are performed as the control. It is demonstrated that without any other treatment, the Au/C shows the highest acetylene conversion of 83.01% while has the obvious deactivation after 24 h of reaction, whose deactivation rate reaches 0.97 h^{-1}. Even the support treated by aqua regia, the conversions over obtained Au/C-AR decrease rapidly from 83.91% to 67.07% within 24 h. When the ligands were added into catalyst preparation, the Au-M_7-$S_{0.5}$/C catalyst shows the highest conversion (97.1%) with the deactivation rate of 0.29 h^{-1} (Fig. 3a, Figs. S6 and S7, and Table S2 in Supporting information). After comparing with other reported Au-based catalysts designed with three strategies (Table S3 in Supporting information), the optimal catalyst with dual ligands shows the superior performance at high GHSV of C_2H_2. Besides, the selectivity is also considered for both prepared catalysts (Fig. 3b, Figs. S6 and S7, and Table S2). The selectivity of both prepared catalysts is more than 99.0% but when the single ligand M is coordinated with Au-based catalyst, there is an obvious selectivity loss, especially in the catalyst with high mole ratio of ligand S. After the second ligand S addition, the selectivity loss is clearly inhibited. The optimized catalyst shows more than 99.5% of selectivity to VCM and there is no obvious decrease, which is similar with Au/C-AR. Based on the above results, we demonstrate that the addition of these two ligands to the Au-based catalyst can promote the catalytic performance and facilitate the reaction.

To clarify the role of these two ligands over Au-based catalyst during the reaction, the properties of spent catalyst were investigated and analyzed. The particle size analysis of the active component in the catalyst was performed by TEM (Fig. 4a). For the Au-M_7-$S_{0.5}$/C catalyst, the dispersion of Au species is still uniform with a size of 2.67 nm, which is closed to the relative fresh catalyst. While without protected ligands, the particles of Au species over Au/C are obviously aggregated and increases to 12.5 nm (inset of Fig. 4a). Also, the sizes of Au species over spent Au-M_7/C and Au-$S_{0.5}$/C are compared to further determine the role of ligands in Au species aggregation. When the single ligand M is coordinated with Au, the size of Au species remains unchanged before and after reaction (Fig. S8 in Supporting information). But due to the faint electrostatic interaction between Au species and ligand S, the Au species over Au-$S_{0.5}$/C shows an obvious increase from 3.30 nm to 4.78 nm (Fig. S9 in Supporting information). The above results demonstrate that the ligand M coordinated with Au species plays a dominated role in inhabitation of active sites aggregation. The XRD patterns are analyzed to further confirm whether the active sites aggregation over catalysts (Fig. 4b). Compared with the fresh catalysts, the intensity of 111 peak associated with Au bulk in patterns of spent Au/C and Au-$S_{0.5}$/C obviously increases while that in Au-M_7-$S_{0.5}$/C and Au-M_7/C remains nearly unchanged after reaction, indicating the main positive role of ligand M in inhabitation of active sites aggregation.

Thermogravimetry/differential thermogravimetry (TG/DTG) curves were employed to analyze the coke deposition on the catalyst surface during the reaction (Fig. S10 in Supporting information). All the values of coke deposition can be quantificationally calculated through the mass loss of fresh and spent catalyst within the temperature range of 150-475 °C. The coke depositions over both catalysts and relative support are considered during the reaction (Fig. 4c). We can see that the coke deposition of pristine Au/C and Au-M_7/AC are both more than ~2.3%, suggesting that the introduction of single ligand M has little inhabitation of coke formation. Interestingly, with electrostatic bonding with ligand S, the coke over Au-$S_{0.5}$/C rapidly decreases to 0.9%. Moreover, when the ligand S is introduced into Au-M_7/C, the obtained catalyst shows the least amount of coke deposition (0.1%) during the reaction. This lower coke deposition demonstrates that this weak interaction is beneficial for coke removal during the reaction. Then, we define the specific area loss (ΔS_{BET}, Fig. 4d) calculated from low temperature N_2 adsorption-desorption isotherms (Fig. S11 and Table S4 in Supporting information) to further determine the

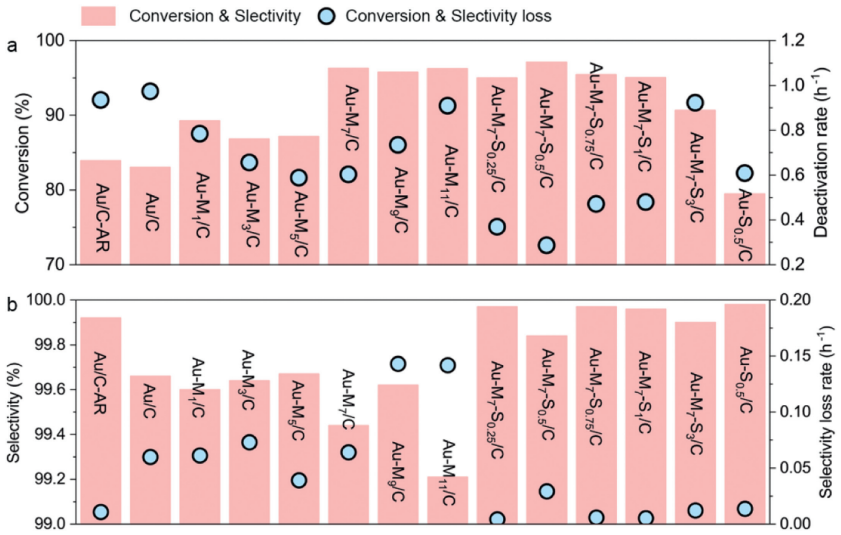

Fig. 3. (a) The acetylene conversion and (b) selectivity to VCM in a packed-bed reactor. Reaction conditions: temperature = 180 °C, GHSV (C_2H_2) = 720 h^{-1}, and $V_{HCl}/V_{C_2H_2}$ = 1.15.

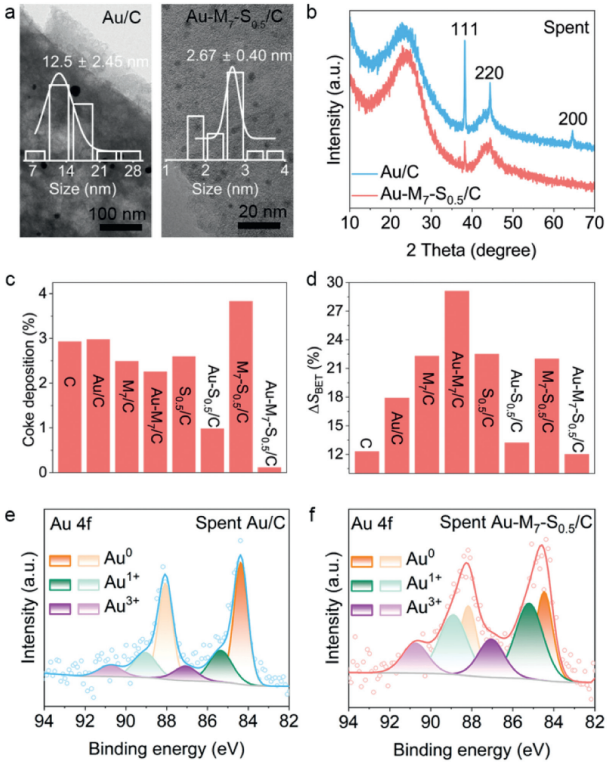

Fig. 4. HRTEM images of (a) spent Au/C and Au-M_7-$S_{0.5}$/C; The inset is the size analysis of Au species. (b) XRD patterns of spent Au/C and Au-M_7-$S_{0.5}$/C. (c) coke deposition and (d) ΔS_{BET} of prepared catalysts. Au 4f region of spent (e) Au/C and (f) Au-M_7-$S_{0.5}$/C.

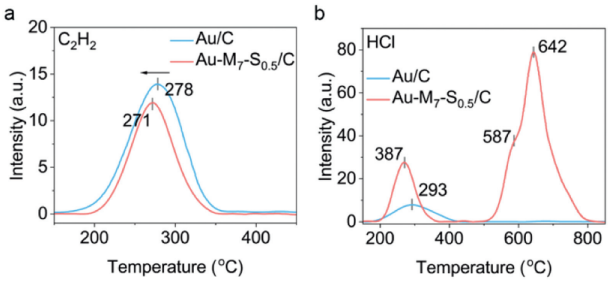

Fig. 5. (a) C_2H_2-TPD and (b) HCl-TPD profiles of the fresh Au catalysts.

coke deposition. We demonstrate that the Au-M_7-$S_{0.5}$/C catalyst has the lowest ΔS_{BET} with the value of 12.0%, which is closed to pristine activated carbon (12.0%). That is, the specific area loss of Au-M_7-$S_{0.5}$/C catalyst originates from the carbon support rather than the metal active sites, which is beneficial to react stably. Besides, the chemical state of Au species for spent Au/C and Au-M_7-$S_{0.5}$/C are analyzed to determine whether the Au^{n+} can be reduced or not during the reaction (Figs. 4e and f, Table S1). After reaction, near 67.1% of Au^{n+} species still exist in Au-M_7-$S_{0.5}$/C, which is 11.3% more than the fresh catalyst. That is, the Au^{n+} species protected by two ligands is stable even under the reduced reaction atmosphere. Based on the above results, we demonstrate that the introduction of two ligands over Au/C is beneficial for the inhibition of Au nanoparticles aggregation, coke deposition and Au^{n+} species reduction, which can enhance the activity and stability of Au-based catalyst.

To further determine the reason of activity enhancement, programmed temperature desorption (TPD) under reaction atmosphere were employed to reflect the adsorption capacity and desorption temperature of the catalyst. The desorption of fresh catalysts to C_2H_2 occurred in the range of 150-400 °C (Fig. 5a). By comparative analysis, it is found that the amount of adsorbed acetylene over fresh Au/C is much higher than that over ligand-protected gold-based catalyst. More importantly, higher desorption temperature and larger peak width of Au/C indicate that the introduction of ligands can inhibit the excessive adsorption of acetylene and promote the rapid desorption of acetylene over active sites, thus decreasing the accumulation of coke. As for the reactant of HCl, the desorption temperatures in fresh Au/C appears at 293 °C and this wide range of 150-400 °C illustrates the slow desorption of HCl on the surface of Au/C (Fig. 5b). When the dual ligands are introduced into catalyst, three obvious desorption peaks with high intensity appear at 267, 587 and 642 °C, respectively. That is, more HCl molecules are adsorbed on the surface of catalyst compared with pristine Au/C, which promotes the reaction rate. According to the results of catalysts with single ligand (Fig. S12 in Supporting information), this improvement of peak at 267 °C is attributed by the synergistic effect of dual ligands while the peaks at high temperature are affected by the ligand M. From the results analysis of

TPD, we demonstrate that this dual-ligand engineering optimizes the desorption behavior of reactants.

In summary, two types of ligands including a molecular 2-methylimidazole and an ionic cetrimonium were introduced in the preparation of Au-based catalyst. With the coordination of 2-methylimidazole and electrostatic interaction of cetrimonium, the Au^{n+} species are stable during the reaction without reduction and agglomeration. Through analyzing the properties of fresh and spent catalysts, we demonstrated that the existence of molecular ligand greatly increases the adsorption of hydrogen chloride while the ionic ligand significantly inhibits the deposition of coke. Based on the positive effect of dual-ligands, we achieve 97.1% highest conversion of acetylene and 0.25 h^{-1} deactivation rate under the GHSV(C_2H_2) of 720 h^{-1}. This work establishes a foundation to explore the property-activity relationships in Au-based catalyst *via* ligand engineering.

Declaration of competing interest

We declare that we do not have any commercial or associative interest that represents a conflict of interest in connection with the work submitted.

CRediT authorship contribution statement

Yongsheng Xu: Writing – review & editing, Writing – original draft, Supervision, Methodology, Investigation, Conceptualization. **Lisha Yao:** Writing – original draft, Software, Methodology, Investigation, Conceptualization. **Jian Li:** Writing – review & editing, Investigation, Funding acquisition. **Yanzhao Dong:** Writing – review & editing, Investigation. **Dongyang Xie:** Writing – review & editing, Investigation. **Miaomiao Zhang:** Writing – review & editing, Investigation. **Feng Li:** Writing – review & editing, Investigation. **Yunsheng Dai:** Writing – review & editing, Visualization, Validation, Supervision, Methodology, Funding acquisition. **Jinli Zhang:** Writing – review & editing, Visualization, Validation, Supervision. **Haiyang Zhang:** Writing – review & editing, Visualization, Validation, Supervision, Methodology, Funding acquisition, Conceptualization.

Acknowledgments

This work was supported by the National Natural Science Foundation of China (No. 22068031), Yunnan Precious Metals Laboratory Science and Technology Project (No. YPML-2022050237), Major Science and Technology Project of Yunnan Precious Metal Laboratory (No. YPML-2023050202), the Science and Technology Project of Xinjiang Bingtuan supported by Central Government (No. 2022BC001), Tianshan Talents Training Program of Xinjiang Science and Technology Innovation Team (No. 2022TSYCTD0021), the Start-Up Foundation for Young Scientists of Shihezi University (No. RCZK202419) and the Project of Achievement Transformation and Technology Extension of Shihezi University (No. CGZH202302).

Supplementary materials

Supplementary material associated with this article can be found, in the online version, at doi:10.1016/j.cclet.2024.110318.

References

[1] G. Malta, S.A. Kondrat, S.J. Freakley, et al., Science 355 (2017) 1399–1403.
[2] J. Li, H. Zhang, M. Cai, et al., Appl. Catal. A 592 (2020) 117431.
[3] X. Zhou, S. Xu, Y. Liu, et al., Mol. Catal. 461 (2018) 73–79.
[4] G.J. Hutchings, J. Catal. 96 (1985) 292–295.
[5] A. Lazaridou, L.R. Smith, S. Pattisson, et al., Nat. Rev. Chem. 7 (2023) 287–295.
[6] X. Wang, G. Lan, H. Liu, et al., Catal. Sci. Technol. 8 (2018) 6143–6149.
[7] B. Wang, Y. Yue, C. Jin, et al., Appl. Catal. B 272 (2020) 118944.
[8] S.K. Kaiser, E. Fako, G. Manzocchi, et al., Nat. Catal. 3 (2020) 376–385.
[9] X. Xu, J. Zhao, C. Lu, et al., Chin. Chem. Lett. 27 (2016) 822–826.
[10] C. Zhao, X. Qiao, Z. Yi, et al., Phys. Chem. Chem. Phys. 22 (2020) 2849–2857.
[11] Y. Wu, F. Li, J. Xue, et al., Chem. Eng. Commun. 207 (2019) 1203–1215.
[12] L. Lian, L. Wang, H. Yan, et al., J. Mater. Res. Technol. 9 (2020) 14961–14968.
[13] X. Dong, C. Zhao, Q. Guan, et al., Appl. Organomet. Chem. 32 (2018) e4570.
[14] X. Qiao, Z. Zhou, X. Liu, et al., Catal. Sci. Technol. 9 (2019) 3753–3762.
[15] S.K. Kaiser, R. Lin, S. Mitchell, et al., Chem. Sci. 10 (2019) 359–369.
[16] Y. Lu, F. Lu, M. Zhu, J. Taiwan Inst. Chem. Eng. 113 (2020) 198–203.
[17] H. Zhang, B. Dai, X. Wang, et al., Green Chem. 15 (2013) 829–836.
[18] M. Conte, C.J. Davies, D.J. Morgan, et al., Catal. Sci. Technol. 3 (2013) 128–134.
[19] X. Chen, X. Qin, Y. Jiao, et al., Nat. Commun. 14 (2023) 2588.
[20] F. Huang, M. Peng, Y. Chen, et al., J. Am. Chem. Soc. 144 (2022) 18485–18493.
[21] J. Peng, X. Yin, D. Dong, et al., Chin. Chem. Lett. 35 (2024) 109508.
[22] B. Wang, L. Yu, J. Zhang, et al., RSC Adv. 4 (2014) 15877–15885.
[23] Y. Jia, R. Hu, Q. Zhou, et al., J. Catal. 348 (2017) 223–232.
[24] X. Di, J. Zhao, Y. Yu, et al., Chin. Chem. Lett. 27 (2016) 1567–1571.
[25] X. Yin, C. Huang, L. Kang, et al., Catal. Sci. Technol. 6 (2016) 4254–4259.
[26] Y. Li, C. Zhang, H. Zhang, et al., Appl. Catal. A 612 (2021) 118015.
[27] P. Johnston, N. Carthey, G.J. Hutchings, J. Am. Chem. Soc. 137 (2015) 14548–14557.
[28] J. Zhao, S. Gu, X. Xu, et al., Catal. Sci. Technol. 6 (2016) 3263–3270.
[29] R.S. Dawson, S. Pattisson, G. Malta, et al., Small 17 (2021) 2007221.
[30] J. Zhao, S. Wang, B. Wang, et al., Chin. J. Catal. 42 (2021) 334–346.
[31] C. Zhang, H. Zhang, Y. Li, et al., ChemCatChem 11 (2019) 3441–3450.